Probing the interface potential in stick/slip friction by a lateral force modulation technique

Kerssemakers, J.W J; De Hosson, J.T.M.

Published in:
Surface Science

DOI:
10.1016/S0039-6028(98)00672-4

ELSEVIER

Surface Science 417 (1998) 281–291

surface science

Probing the interface potential in stick/slip friction by a lateral force modulation technique

J. Kerssemakers, J.Th.M. De Hosson *

Department of Applied Physics, Materials Science Center, University of Groningen, Nijenborgh 4, 9747AG Groningen, The Netherlands

Received 27 February 1998; accepted for publication 13 August 1998

Abstract

The influence of the shape of the interaction potential is investigated on details in stick/slip friction as encountered between an AFM tip and a substrate. Based on qualitative arguments of stick/slip systems, a novel technique is introduced in which the AFM tip is brought into a lateral resonance mode. In comparison to a direct measurement in the stick/slip signal, we suggest that the method is preferable to highlight these non-linear characteristics. In combination with the shape of the surface potential involved in stick/slip friction, this modulation diminishes the friction loop amplitude in a controlled way. Furthermore, a partial stick/slip behavior is observed above a certain threshold level of driving amplitude, where the tip alternates periodically between a zero-friction and a non-zero-friction state. © 1998 Elsevier Science B.V. All rights reserved.

Keywords: Adhesion; Atomic Force Microscopy; Friction; Sticking; Surface electronic phenomena; Tribolog

1. Introduction

Since its advent, atomic force microscopy (AFM) has made an impetus to a broad range of applications [1]. One of these is friction force microscopy (FFM) [2], in which attention is focused on the force components parallel to the substrate plane, on an atomic scale [3]. Interpretation of friction in a physical sense is not straightforward. Although recent work has resulted in calibration routines to obtain quantified friction data [4], the physical, or more specifically, the atomistic processes leading to friction are not always transparent. Numerous studies on general stick/slip friction introduce different descriptive models [5], the parameters of which may be linked to physical microscopic components of the slider–substrate system [6]. In the case of AFM stick/slip phenomena, recent work has led to a link between friction and deformation [7] in the well-known phenomenon of two-dimensional stick/slip friction [8].

This link of stick/slip friction and deformation is typically observed on materials possessing a layered structure. The choice of materials to investigate was driven by this structural aspect, with extra attention to the transition metal dichalcogenides (TMX). These TMX materials. like TiS_2, exhibit strong atomic periodicity when imaged by AFM. Transition-metal dichalcogenides exhibit a remarkable two-dimensional behavior, despite their three-dimensional atomic structure. The crys-

* Corresponding author. Fax: +31 503634881;
e-mail: hossonj@phys.rug.nl

PII: S0039-6028(98)00672-4

tallographic structure can be described as a hexagonal close-packed layer of transition metal atoms (Ti, Nb, W), sandwiched in between two layers of chalcogen atoms (S, Te, Se) with the same symmetry. Unit cells MX_2, in which M represents the transition metal and X represents a chalcogen, are connected by relatively strong chemical bonds within the sandwich but only weakly bonded to adjacent sandwiches. Because of this particular atomic arrangement, the physical properties exhibit a rather strong anisotropic behavior. In the past, extensive scanning tunneling microscopy (STM) and atomic force microscopy (AFM) studies on these materials have been carried out. Observed effects are charge density waves (CDW) [9] and pinning of CDW by point defects by STM as well as periodic lattice distortions (PLD) [10] by AFM and more recently a measurable deformation occurring during stick/slip friction [11].

In AFM, stick/slip friction the AFM tip jumps between discrete sites in a strongly jerky fashion while it is pulled along the substrate [8]. In most cases, these sites reflect the lattice periodicity of the substrate (Fig. 1). It is noted that the interaction area between tip and substrate during this process is typically tens of nanometers in diameter, which implies that the observed atomic periodicity is not real atomic resolution but a collective process of many breaking and rebonding atomic bonds.

In most friction processes, this breaking and debonding averages, leading to a smooth friction force, from which it is hard to extract physical quantities on the atomic processes. However, the collective character of a stick/slip event provides an insight of the friction process at an atomic scale.

A complicating factor forms the two-dimensional nature of AFM stick/slip friction, i.e. the tip is not necessarily moving in the direction of the pulling force. The complex slip patterns performed by the tip turn out to be primarily governed by one single material property, namely the maximum lateral strain, ϵ_0, which can be exerted on the stuck tip/substrate interface. For a specific cantilever with an anisotropic lateral stiffness $k_c(\alpha)$, this length is directly linked to the maximum force or initial sticking by $\epsilon_0 = F_{max}/k_c(\alpha)$, which is the distance the cantilever system can be strained before it jumps. Here, α expresses the lateral direction of scanning with respect to one main axis of the substrate lattice (see also Fig. 2). In combination with the lattice length, λ, the parameters ϵ_0 and α allow for an exact description of the stick/slip patterns in terms of tip strain coordinates (ϵ_x, ϵ_y), as shown in Fig. 2 [12].

Thus, the two-dimensional character of stick/slip is governed by the one-dimensional parameter ϵ_0, which in turn is closely linked to the static friction. Therefore, we will restrict the following part to a one-dimensional approach. Experimentally, this situation is obtained if the tip is pulled along a main axis of the surface-lattice, provided that scans with zigzag movements are excluded from the analysis [12].

For layered materials, the maximum strain length ϵ_0 turns out to be divided over the cantilever as well as the substrate. The lateral strain of the cantilever is commonly recognized as cantilever buckling when it is directed along the length axis of the cantilever and as torsion if the strain is directed perpendicular to this axis. The strain in the substrate leads to a surface stiffness for a given contact area. This stiffness is typically of the same order as, or even lower than, the lateral stiffness of the cantilever, which is of the order $102\ N\ m^{-1}$ [13]. It should be noted that the concept of a single constant stiffness is a strong simplification, for which the applicability should always be verified. In a former study, it turned out that layered materials indeed behave as virtually linear springs, but that on other materials, this concept does not hold [14]. Therefore, at present, we interpret the deformations in the contact area and below in a different view, namely that of a periodic force interaction between the tip and substrate. The origin of this force interaction may lead to two different interpretations. The first and simplest is the existence of a periodic and conservative interaction potential, that can be summed on the spring potential of the cantilever (Fig. 3a). This approach is mostly followed in explanations of stick/slip processes [15–20]. As long as the minima of such a potential are not infinitely sharp, the tip will always perform some precursor sliding before the actual slip occurs. This sliding causes a

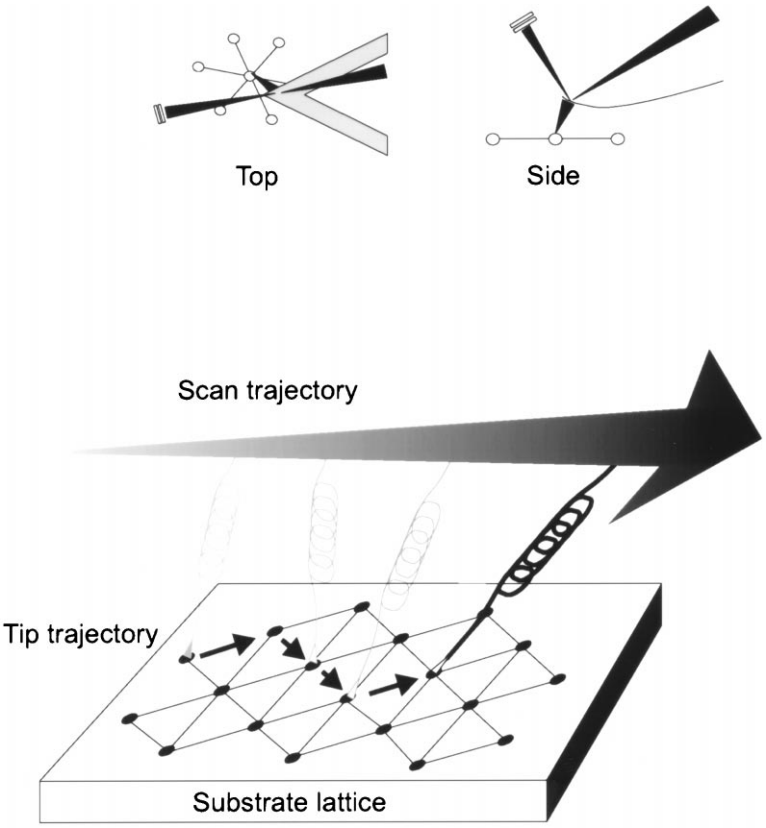

Fig. 1. Discrete modeling of the AFM stick/slip system. Upper: AFM configuration. Only lateral movements are considered. Lower: two-dimensional stick/slip friction. Although, on average, the one (tip) end of the spring should follow the other pulled end, the actual motion can be quite different.

reduction of the measured cantilever lateral deflection. It should be noted that this approach is physically equivalent to the concept of a (non-)linear stiffness of the surface [11,13,21].

A more phenomenological approach suggests irreversible micro-slips of atomic bonds between the tip and surface. In this second view, the only difference between a stick and a slip phase is the number of micro-slips that occur during a small increase of cantilever displacement. This second view is probably more applicable in the case of layered materials [22] where the collective straining of bonds leads to a strong linear substrate deformation during the sticking phase [11,13,21]. In a more general case, the stick/slip is governed by a mix of conservative and irreversible processes

2. Potential dependence of stick/slip friction

For the sake of clarity, here, we propose the existence of a substrate-bound periodic interaction potential.

Our starting point is the equation

$$m\ddot{x}+k_c(x-v_0t)+D(x,\dot{x})+P'(x)=0, \qquad (1)$$

where k_c is the lateral stiffness of the cantilever, and m is the effective weight involved in small lateral displacements of the cantilever tip. $D(x,\dot{x})$ is a general damping term depending on position x and the speed. $P'(x)$ expresses a conservative periodic surface potential. Simulations based on similar analytic approaches were performed in

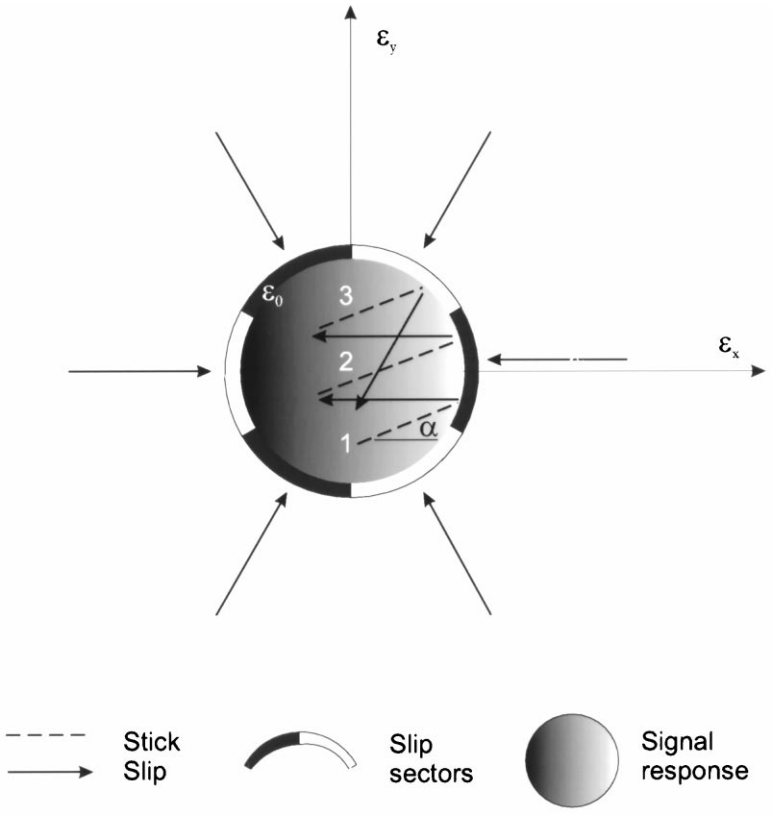

Fig. 2. Geometrical modeling of two-dimensional stick/slip friction. Coordinates (ϵ_x,ϵ_y) represent tip displacement from the (0,0) fully relaxed tip position. Possible lattice translations or slips are marked by arrows. One such slip is most favorable in one angular segment, the "slip sectors". The shading gradient represents the linear detector signal at any point (ϵ_x,ϵ_y). Slip occurs any time that $|\epsilon|=\epsilon_0$. Any route is described by a sequence of scanning and jumping vector translations, which, by definition, never cross the threshold circle. The relative size of the threshold circle governs the complexity of the stick/slip patterns.

literature to describe the influence of model parameters on image formation [15–20].

In Fig. 3a–c, the behavior of this system is visualized in a one-dimensional fashion. In this concept, the maximum strain ϵ_0 is at the point "A" in Fig. 3a–c, where we find:

$$\epsilon_0 = \frac{P'(\epsilon_0)}{k_c}, \quad \text{with } k_c = P''(\epsilon_0). \tag{2}$$

Eq. (2) denotes the situation just prior to slip. More straining results in the disappearing of the equilibrium point at "A" in Fig. 3a, after which the tip accelerates, dissipates and stops in a more relaxed minimum, which can be "B", but also "C" in Fig. 3a. From this simplified energy picture, the influence of the shape of the interface potential is not very clear. Nevertheless, from Eqs. (1) and (2), we learn that the static friction is clearly not dependent on the depth of the interaction potential $P(x)$, but on its shape.

The effect of potential shape on stick/slip becomes more clear in its derivatives, as shown in Fig. 3b. Here, the force balance of the cantilever and interaction field is shown by the crossing point of both force-displacement graphs [15]. Scanning causes the origin of the cantilever line to shift relative to the interaction curve. A stable equilibrium is only possible in the substrate areas denoted by a thick solid curve. These parts fulfill the condition that the derivative of the interaction force field exceeds k_c, the derivative of the cantilever force field. Therefore, the existence and magni-

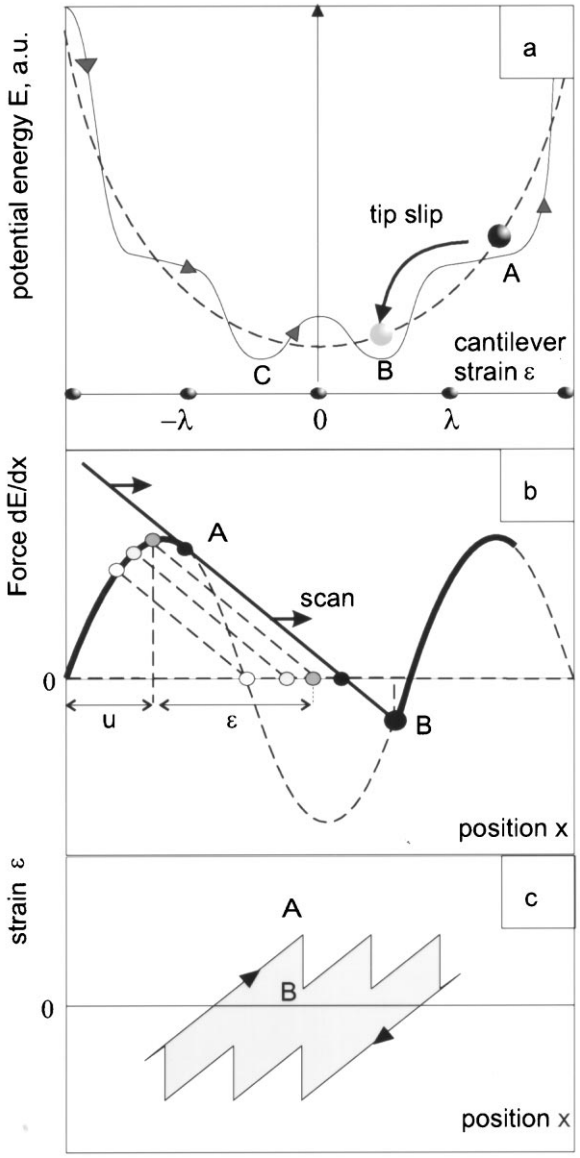

Fig. 3. Conceptual view of a one-dimensional stick/slip system. (a) Energy plot of periodic stick/slip. The origin expresses zero cantilever strain. A periodic interaction tip–substrate potential, P, exists with period, λ. Scanning translates this potential relative to the parabolic potential of the cantilever itself (dotted line). The total time-dependent potential energy is then expressed by the solid line with arrows. The tip position is denoted by a sphere. It moves along with a minimum, A, in total energy, until this disappears, upon which, slip follows to minimum B or C. (b) Force view of a stick/slip process. The time-dependent cantilever force on the tip is expressed by the solid and dotted straight lines. The zero-crossing of these lines expresses the moving free rest position of the cantilever in time. The relative position of interaction force field $P(x)$ is expressed by a static sinusoidal curve with period, λ. Crossing points of lines and sinusoid express stable equilibrium positions of the tip. At any time, the tip strain is expressed by ϵ. These stable points only exist along the thick line pieces of the sinusoid. Dotted line pieces along the sinusoid express unstable positions. Slip occurs at the end points of stable regions, from A to B. Thus, u is the distance the tip actually moved in a quasi-static fashion since the last slip. (c) Stick/slip signal. As only the cantilever strain, ϵ (see Fig. 3b), can be detected, it is this parameter that is actually seen in the well-known stick/slip friction loops. The larger the sliding of the tip between slips (u in Fig. 3b), the smaller this detected strain will be.

tude of the slip depends on the stiffness, k_c, of the cantilever in combination with the stiffness of the interaction force field. A slip here consists of an instantaneous translation from "A" to "B". Also shown as shaded dots in Fig. 3b are some arbitrary stable tip positions for different corresponding positions of the cantilever base. Precursor sliding of the tip is denoted by u, and the cantilever strain is given by the distance ϵ. In a friction loop, as in Fig. 3c, the precursor sliding is recognized as the difference between the theoretical signal yield and that actually measured [11,13,21].

Within this model and the construction routine, as described in Fig. 3b, different interaction potential shapes lead to qualitatively different stick/slip traces This is clarified in Fig. 4. Shown for some different interaction potentials (I–IV) are: (a) the potential shape, (b) the construction set up analogously to Fig. 3b, and (c) the resulting friction signal as it would be measured. In Fig. 4c-I, c-II and c-IV, two different cantilever stiffnesses (solid and dotted lines) lead to qualitative differences in strong- and weak frictional behavior), leading to different friction signals for both cases, as shown in Fig. 4c:

(I) See Fig. 4-I. For a sinusoid, a stiff cantilever leads to a weak sinusoidal variation of the friction signal (dotted lines), whereas a soft cantilever results in a slightly rounded sawtooth signal (solid lines). This type of potential should be expected for simple, rigid surface lattices when, for instance, a Lennard–Jones potential could be applied [18].

(II) However, in the case of a collective deformation beneath the tip–substrate interface combined with a rather strongly bonded tip, a potential as in Fig. 4-II is more appropriate. This should be expected for weak substrates or strong chemical binding between tip and substrate. Sawtooth-like stick/slip will be present for any cantilever stiffness, although the slope of this sawtooth will be lowered as compared to a completely fixed tip. This type is known from stick/slip in ambient air on layered substrates [8].

(II) See Fig. 4-III. Stiff coherent lattices of tip

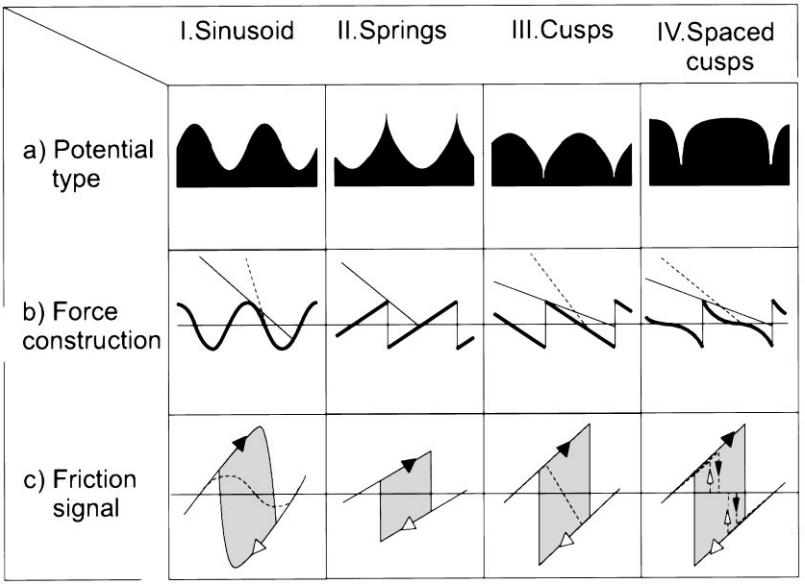

Fig. 4. Influence of potential shape on friction loops in energy plots (a), force plots (b) and friction signals (c). For a detailed explanation, see Fig. 3. Different potential types in (a) lead two different force constructions in (b). The dotted lines correspond to relatively stiff cantilevers, which can lead to qualitatively different frictional behavior (c), depending on the potential type. See also main text.

and surface under high pressure may lead to an effective cusp-like interaction potential, where any deformation leads to a weakening of the bonding between tip and surface. Soft cantilevers lead to "perfect" stick/slip friction, whereas stiff cantilevers will show perfect sticking alternated by a constant yielding.

(IV) If the cusps in a potential like in Fig. 4-III are relatively sharp, i.e. a rather flat potential exists in between the cusp sites, some special behavior is expected for sufficiently stiff cantilevers: the cantilever tip will always stick to the surface, but will alternate between sticking and almost free (frictionless) sliding until it is "caught" by the next cusp site.

It can be seen that the physical origin of tip–surface interaction may lead to a rather different frictional behavior. Therefore, it is of great interest to scrutinize the shape of the sticking phase as well as its absolute slope as compared to that of an rigidly fixed tip. Such a fixed tip will yield a maximum signal sensitivity (in units of signal per nm strain) when strained. To accomplish this comparison, it is necessary to determine the value of the upper yield.

3. Experimental

It has been shown that the theoretical maximum of signal sensitivity can be determined analytically [11], as well as experimentally [13]. A direct measurement of the sticking signal is feasible, and may lead to a strain-dependent compliance [14]. A problem with this approach is the rather high signal-to-noise ratio of a stick/slip signal ($\sim$5:1), as measuring a strain-dependent compliance involves taking the derivative of the stick/slip signal. To obtain an acceptable error margin in this derivative, it is necessary to average a large ($\sim$20) number of scanlines. This averaging opposes the goal of obtaining information of details in the strain characteristics, as the lack of a physically clear reference point in each curve hinders a proper summation of comparable points on each individual strain curve.

Therefore, we propose the following method. We manipulate the stick/slip system in a physically sound sense, and make use of the associated decrease in the maximum width of the friction loop, which is the distance of the sawtooth tops between the forward and backward scans as displayed in Fig. 4cI–IV. This width is coupled to a point of release, analogously to the point of slip given by Eq. (2) and denoted by "A" in Fig. 3.

The basic idea of the method is that the friction loop is clipped at a variable amplitude, without affecting the lower part of this signal. Then, any point on the friction loop can if desired be tuned to be the maximum force, which is easily and reliably measured from the maximum signal amplitude. The advantage of this approach is that the friction loop width is the parameter of interest as well as its own reference point.

To accomplish this experimentally, we apply a high-frequency lateral modulation to the tip, as shown in Fig. 5. As long as the field is not too strong, the tip is constrained in vertical directions by the surface. Then, the cantilever is excited in a sliding-fixed resonance mode [23]. We presume that this lateral movement "dx" is hardly affected by the force the substrate exerts on the tip. This is reasonable because it is well known that the stiffness of the cantilever in lateral directions exceeds the vertical stiffness roughly by two orders of magnitude [24]. This means that the influence of substrate forces on the cantilever in comparison with the electrostatic forces is diminished with a similar factor. Therefore, we interpret the distance dx as only depending on the driving field amplitude.

When the electrostatic field is modulated, the tip is thought to "scan" a range 2dx around its equilibrium point. This changes the situation as depicted in Fig. 3 to that depicted in Fig. 6. The stiff high-frequency modulation of the tip may be visualized with a broadening of the line associated with the cantilever force. As shown, this causes the point of slippage to occur earlier, at point A′ in Fig. 6b. Due to the high frequency, we presume that the average position of the tip at lower strains is still denoted by the thick solid curve. The change in the friction loops is schematically shown in Fig. 6c. The loop is clipped at a specific amplitude. As the modulation amplitude is varied, the friction curve is "scanned" along, and each point, u, as in

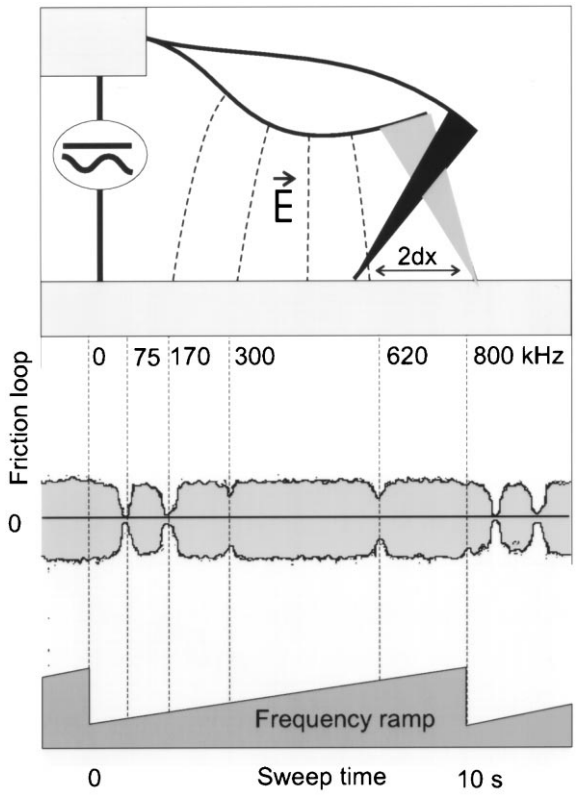

Fig. 5. Upper: application of an electrostatic field, E, between a gold-coated cantilever and the (conducting) sample. This results in lateral modulation, 2dx, of the constrained cantilever tip. Lower: the top–top friction loop signal vs. time is shown during a 10-s frequency sweep. "Gaps" of lowered or eliminated friction at specific frequencies can be observed. The gaps are seen to reproduce, and are presumed to correspond to lateral resonance states of the cantilever.

Fig. 3b can be easily measured from the average maximum signal.

4. Results and analysis

The lateral modulation method is illustrated with some experiments on NbS_2. Modulation of the cantilever was performed in two ways: either a high-frequency X-modulation was summed on the piezo scanner voltage, or electrostatic loading was applied. This was done by modulation an electrostatic field between a sample and a cantilever coated with a few nanometers of Pd or Au. The

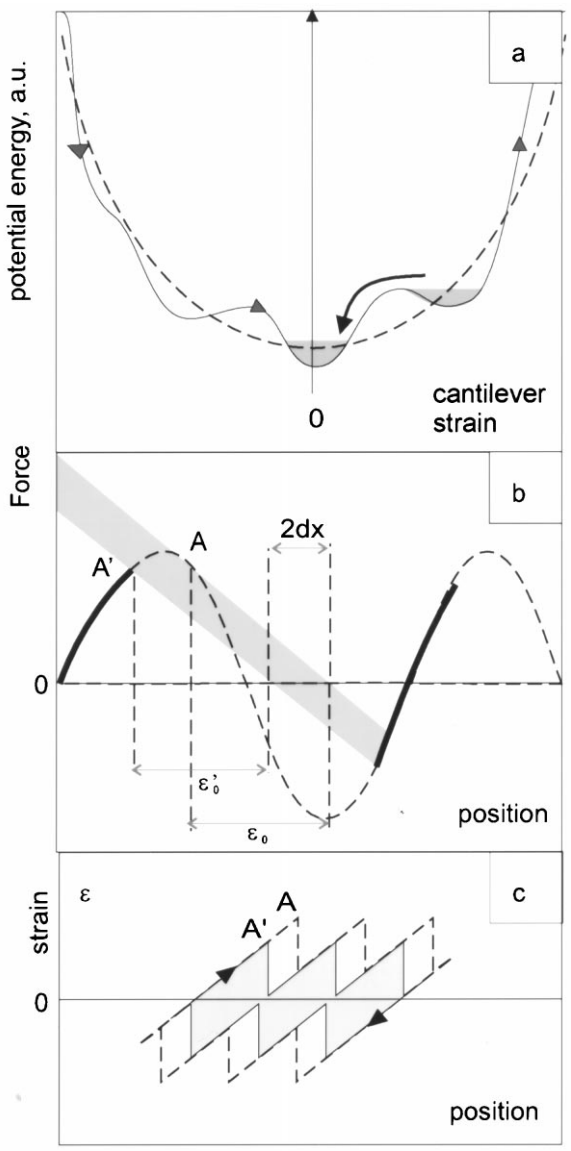

Fig. 6. (a) Energy, (b) force and (c) signal view of a partially suppressed stick/slip process. See also Fig. 3 for a detailed explanation. (a) At a friction gap as shown in Fig. 5, the lateral oscillation causes the tip to perform high-frequency movements in the relatively quasi-static tip–substrate system. This results in premature slip. (b) In the force equilibrium view, the oscillation can be represented by changing the tip line by a shaded ribbon. The tip cannot be strained to point A but instead slips at point A′. (c) The average low-frequency position of the tip reflects a clipped friction loop.

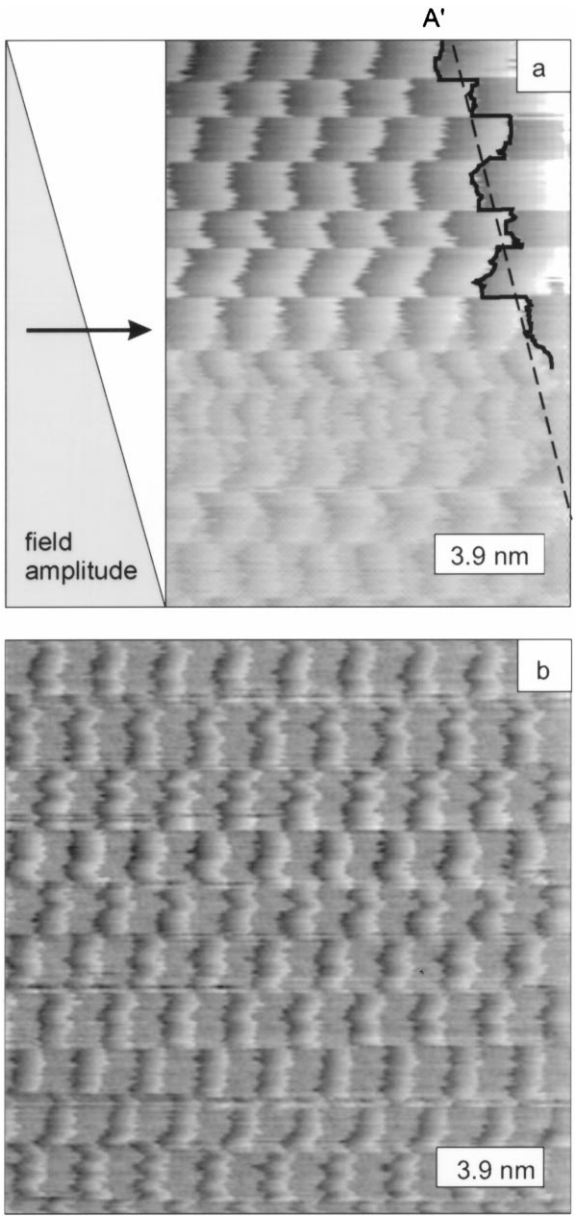

Fig. 7. (a) At a particular friction gap frequency, as visible in Fig. 5, a slow increase in driving field amplitude causes a gradual decrease in friction. The equivalent change of the slip point A′ is marked by the solid line to the right of the image. From a certain strength of the driving field, a qualitative difference occurs, marked by the arrow. In (b), the driving amplitude was kept at a constant level above this threshold. A periodic alternation is visible between two states: one a regular, linear varying sticking signal, and one a region of zero signal variation (gray areas). See also Fig. 8.

friction signal was directly measured by a digital storage oscilloscope.

With the electrostatic method, frequencies of up to 1 MHz resulted in a visible and stable decrease in the friction amplitude at a specific frequency band, as shown in Fig. 5. An increase in the driving field amplitude resulted in a broadening of these friction gaps. The gaps are presumed to be around lateral resonating modes of the used cantilever. The resonance frequencies are much higher than the sampling frequency of our Nanoscope II, which is in the range of 1–100 kHz, and proved to be invisible in the images. Therefore, the images reflect the average position of the cantilever tip. However, the presence of the friction gaps proves that the tip is indeed oscillating laterally. The effects on image formation are shown in Fig. 7a. Here, a gradually increased field amplitude was applied at a resonance gap frequency. The experimental equivalencies of the point of slip A′ in Fig. 6 are marked at the right band of the image. The magnitude of A′ clearly decreases. At the higher driving field amplitude, a qualitative change is taking place at the point marked by an arrow. The stability of the friction suppression is visible in Fig. 7b, where a full scan was subjected to a constant tip oscillation above this change threshold. The effect is well tunable, as shown in Fig. 8, in which the field was turned on twice, resulting in clearly different low- and high-friction areas. Two line traces are depicted from both regions, marked (a) and (b). Apart from a decease in static friction, a qualitative difference is observed, with regular stick phases alternating with zero-amplitude traces.

The observed alternating state can be explained within the same physical concept as for Figs. 3 and 6. In Fig. 9a, the oscillation is visualized in the energy view. The two different frictional states are denoted by I and II. Whereas, in Fig. 9a-I, the average tip position will be hardly affected by the walking sinusoid, after some scanning, the tip will stick to one specific minimum, shown in Fig. 9a-II. In Fig. 9b, the oscillation of the cantilever again is depicted as shaded ribbons. Within these ribbons, any position on the crossing interaction curve is equally available for the oscillating tip. Two extreme position are defined for the relative positions of cantilever origin and interaction force

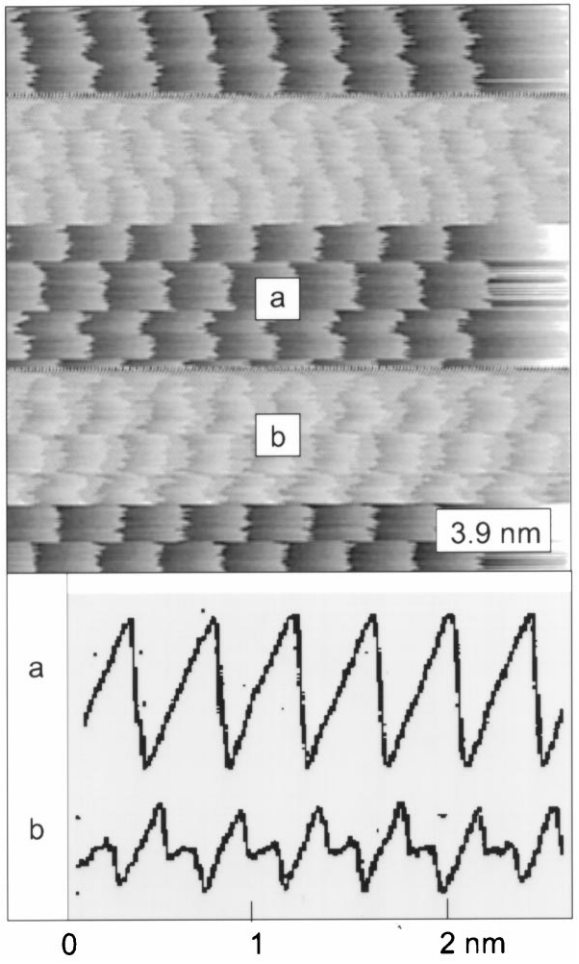

Fig. 8. Double on–off switching of the oscillation, showing the easy controllability and the absence of settling effects in the friction decrease. Two traces (a) and (b) of the different regions both show linearly varying sticking phases. However, in trace (b), they are alternated by zero-signal phases. See also Fig. 7.

field. In the anti-centered state at left, a maximum of the interaction force field coincides with the origin of cantilever strain. Both "snap" points A1 and A2 lie within the shaded area, implying that the tip oscillation exceeds the barrier of the interaction field and thus slips as easily forward as backward. A free state is created in which the cantilever tip freely oscillates around its own origin, creating an average zero deflection. Contrary to this, an anti-centered state is shown on the right, in which a field minimum coincides

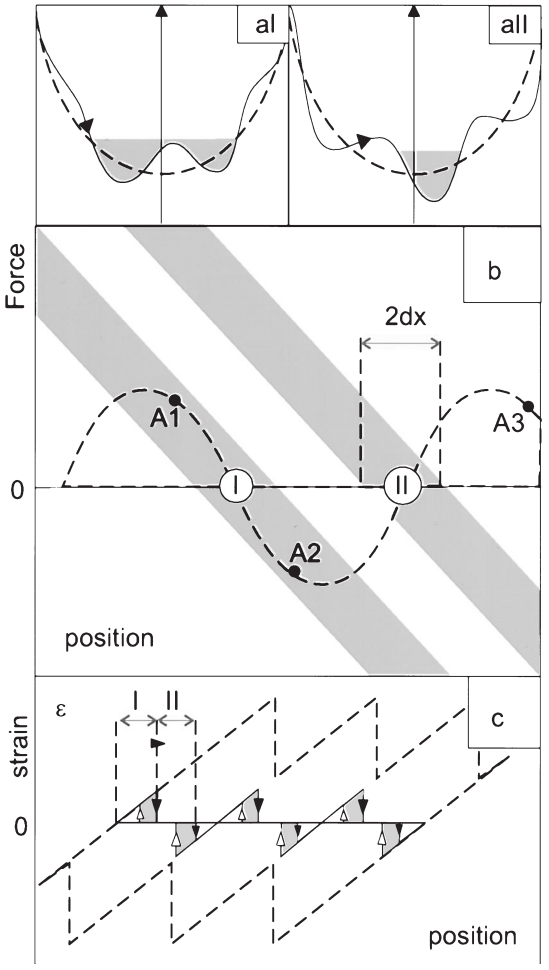

Fig. 9. Explanation of alternating friction as shown Figs. 7 and 8, viewed in energy plots (a), force plots (b) and friction signal (c). See Fig. 3. for an explanation of details. (a) Energy view. The two different frictional states are explained with I and II. In (a-I), the average tip position will be hardly affected by the walking sinusoid for a certain range of positions of the interaction potential relative to the parabolic spring potential. After some scanning, the tip will again stick to one specific minimum, as shown in (a-II). In (b), a combination of signal amplitude and cantilever stiffness (shaded ribbon I) is shown where both forward (A1) and backward (A2) slip points are contained. This corresponds to a relative position of interaction potential and cantilever potential as schematically shown in the upper left graph. As both forward- and backward slip is possible, the average signal of the cantilever is zero. At ribbon (II), another position of the same system does not allow free slip. A range exists where the oscillation is centered around a regular sticking point (solid line). Scanning causes the tip to alternate between these two situations, as shown in (c).

with the field minimum. The same oscillation amplitude is now insufficient to reach the nearby snap points A2 and A3, and a bound state exists with the tip now oscillating around a "regular" equilibrium point, which we observe in the experiment as a non-zero sloped average signal. It is immediately seen that this special behavior only occurs between a minimum oscillation and maximum oscillation amplitude threshold, in combination with a certain value of the cantilever stiffness k_c. In Fig. 9c, it is seen that the friction behavior, as encountered in Figs. 7 and 8, indeed can be produced from this modeling. The fact that this snap-and-catch behavior is indeed observed implies that the actual interaction can at least be described as a periodic, substrate-bound potential and thus supports our model assumptions. Also, a lower limit for complete stick/slip behavior, as introduced in an earlier model description, is shown to be observable in an experimental sense [12].

5. Conclusions

The method of clipping the friction signal is a valuable tool for analyzing linear and non-linear details in stick/slip friction loops. Moreover, the strong discrete nature of the well-known stick/slip on layered materials is further supported by the observation of a partial stick/slip state, proving the existence of a lower limit of slip threshold for a complete stick/slip system.

Acknowledgements

This work is part of the research program of the Foundation for Fundamental Research on Matter (FOM-Utrecht) and has been made possible by financial support from the Netherlands Foundation for Technical Sciences (STW-Utrecht).

References

[1] S.N. Magonov, M.H. Whangbo, Surface Analysis with STM and AFM, VCH, 1996.
[2] Y. Liu, T. Wu, D. Fenell Evans, Langmuir 10 (1994) 2241.
[3] J. Hu, X.-d. Xiao, D.F. Ogletree, M. Salmeron, Surf. Sci. 327 (1995) 358.
[4] D.F. Ogletree, R.W. Carpick, M. Salmeron, Rev. Sci. Instrum. 67 (1996) 3298.
[5] H. Yoshizawa, J. Israelachvili, J. Phys. Chem. 97 (1993) 11300.
[6] T. Baumberger, F. Heslot, B. Perrin, Nature 367 (1994) 544.
[7] R.W. Carpick, N. Agrait, D.F. Ogletree, M. Salmeron, J. Vac. Sci. Technol. B 14 (1996) 1289.
[8] S. Morita, S. Fujisawa, Y. Sugawara, Surf. Sci. Rep. 23 (1996) 1.
[9] C.G. Slough, W.W. McNairy, R.V. Coleman, J. Garnaes, C.B. Prater, P.K. Hansma, Phys. Rev. B 42 (1990) 9255.
[10] Y. Gong, Q. Xue, Z. Dai, C.G. Slough, R.V. Coleman, L.M. Falicov, Phys. Rev. Lett. 71 (1993) 3303.
[11] J.W.J. Kerssemakers, J.Th.M. De Hosson, J. Appl. Phys. 81 (1997) 3763.
[12] J.W.J. Kerssemakers, J.Th.M. De Hosson, J. Appl. Phys. 80 (1996) 623.
[13] R.W. Carpick, D.F. Ogletree, M. Salmeron, Appl. Phys. Lett. 70 (1997) 526.
[14] J.J. Kerssemakers, J.Th.M. De Hosson, Appl. Phys. Lett., submitted.
[15] D. Tomanek, W. Zhong, H. Thomas, Eur. Lett. 15 (1991) 887.
[16] R.M. Overney, H. Takano, M. Fujihira, W. Paulus, H. Ringsdorf, Phys. Rev. Lett. 72 (1994) 3546.
[17] J.W.J. Kerssemakers, J.Th.M. De Hosson, Appl. Phys. Lett. 67 (3) (1994) 347.
[18] N. Sasaki, K. Kobayashi, M. Tsukada, Surf. Sci. 357 (1996) 92.
[19] N. Sasaki, K. Kobayashi, M. Tsukada, Jpn. J. Appl. Phys. 35 (1996) 3700.
[20] H. Holscher, U.D. Schwarz, R. Wiesendanger, Surf. Sci. 375 (1997) 395.
[21] M.A. Lantz, S.J. O'Shea, A.C.F. Hoole, M.E. Welland, Appl. Phys. Lett. 70 (1997) 970.
[22] A. Buldum, S. Ciraci, Phys. Rev. B 55 (1996) 2606.
[23] U. Rabe, K. Janser, W. Arnold, Rev. Sci. Instrum. 67 (1996) 3281.
[24] J.M. Neumeister, W.A. Ducker, Rev. Sci. Instrum. 65 (1994) 2527.